Paper No. 59. (quote when citing this article)
Eleventh World Conference on Earthquake Engineering
ISBN: 0 08 042822 3

EXPERIMENTAL STUDIES ON EMBEDMENT EFFECTS ON DYNAMIC SOIL-STRUCTURE INTERACTION

Y. OHTSUKA
Kobori Research Complex, Kajima Corporation, 6-5-30 Akasaka, Minato-ku, Tokyo 107, Japan.
A. FUKUOKA
Kajima Technical Research Institute, Kajima Corporation, 2-19-1 Tobitakyu, Chofu-shi, Tokyo 182, Japan.
K. AKINO
Nuclear Power Engineering Corporation, 4-3-13 Toranomon, Minato-ku, Tokyo 105, Japan.
K. ISHIDA
Central Research Institute of Electric Power Industry, 1646 Abiko, Abiko-shi, Chiba 270-11, Japan.

ABSTRACT

Soil-structure interaction plays an important role in determining the dynamic characteristics of very massive, stiff structures during earthquakes. Backfill and surrounding soil have significant effects on soil-structure interaction for embedded structures. This paper investigates the inertial and kinematic interactions of embedded structures. Soil impedances and foundation input motions obtained from forced vibration tests and earthquake records are discussed in relation to embedment effects. Experiments were carried out using large scale models to obtain basic data to verify analysis codes. Analytical results using the Axisymmetric FEM model conformed well with the structure responses. These experimental and analytical studies clarified the complicated dynamic properties of embedded structures.

KEYWORDS

Dynamic soil-structure interaction; forced vibration test; foundation input motion; embedment effect; axisymmetric FEM

INTRODUCTION

The seismic response of embedded structures is greatly affected by soil-structure interaction, which is particularly complicated, because of the existence of backfill and surrounding soil. Large-scale models designed in consideration of the fundamental dynamic characteristics of a BWR-type reactor building in Japan were constructed on ground to investigate the inertial and kinematic interactions of embedded structures. Forced vibration tests and earthquake observations were carried out on these models. The experimental and observed results for dynamic soil impedances, foundation input motions , and responses of structures, backfill and surrounding soils were compared using the Axisymmetric Finite Element Method, hereafter called the "FEM" model.

TEST CONDITIONS AND ANALYSIS MODEL

Test Model

To investigate embedment effects on dynamic soil-structure interaction, two reinforced concrete model structures, Model A and Model B, were constructed about 60m apart on a soft rock site, after excavating the ground to 5m depth. A general view of Model B is shown in photograph 1 and a cross section of the models is shown in Fig.1. Each model has an 8m-square foundation. Model A is a box-wall structure without embedment and Model B is identical to Model A, but embedded 5m deep. The total weight of each model structure is about 657ton. The test models were scaled down to about 1/10 in consideration of the fundamental dynamic characteristics of a BWR-type reactor building in Japan (Miyamoto et al., 1991).

Soil Condition

The test models were constructed on ground. According to a boring survey and PS logging, the test site was confirmed to be a layered half-space. In the layer immediately under the foundation bottom, the shear wave velocity was 300m/sec. - 450m/sec., and in the layer more than 7m under the foundation bottom, it was greater than 1350m/sec.. From exploration with elastic waves on the ground surface after excavation, a soft zone was found near the surface of the excavated ground. The soil conditions under the two test models were almost the same. The backfill soil was compacted to produce a homogeneous condition of shear wave velocity and soil density for every 15cm layer. The shear wave velocity of the backfill soil was 130m/sec. near the surface and about 150m/sec. around the foundation bottom.

Method of Experiment

Sinusoidal forced vibration tests were performed using a vibration exciter installed on the roof floor (RF) and 1st floor (1F). The excitation force was controlled so that the soil remained in the linear elastic range. Earthquake observations were also carried out on these models and in the surrounding ground.

Analysis Model

Correlation analyses were made using the Axisymmetric FEM and the 1-dimensional wave propagation theory. Fig.2 shows the analysis model. In the correlation analyses, the basement part was treated as a rigid body based on the measuring mode of the basement, and the structure was assumed as a multi-lumped mass model considering bending and shearing deformation. In the Axisymmetric FEM model, the energy dissipation from the analysis boundary of the finite soil towards the out side was evaluated with the addition of viscous boundary at the bottom boundary and transmitting boundary at the side boundary. The square basement was modeled as an equivalent circular basement with an area equal to that of the square basement. For earthquake response analyses, the outcrop motion (, i.e., double the up-going wave components,) was used as the input at the bottom of the Axisymmetric FEM model. Using the 1-dimensional wave propagation theory, the outcrop motion was evaluated from the observed record at GL-34.3m including up- and down-going wave components. The constants of the soil properties adopted in these correlation analyses are summarized in Table 1. The element numbers in Table 1 are identical to those in Fig.2. These values, except the damping factor, were determined based on the measured data of the PS logging and the exploration with elastic waves at the test site. The damping factors were determined by correlation analyses of dynamic soil impedance functions.

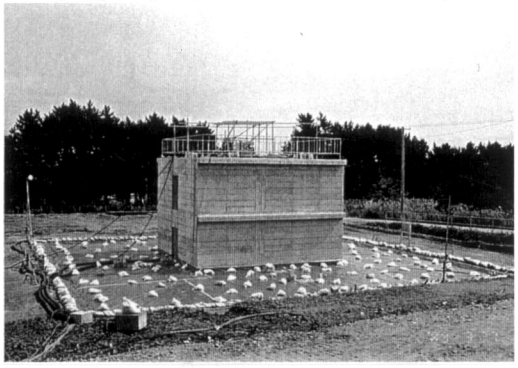

Photograph 1. Test model B

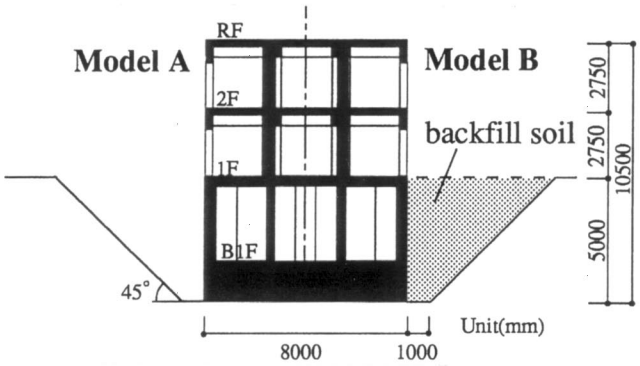

Fig.1. Cross section of test models

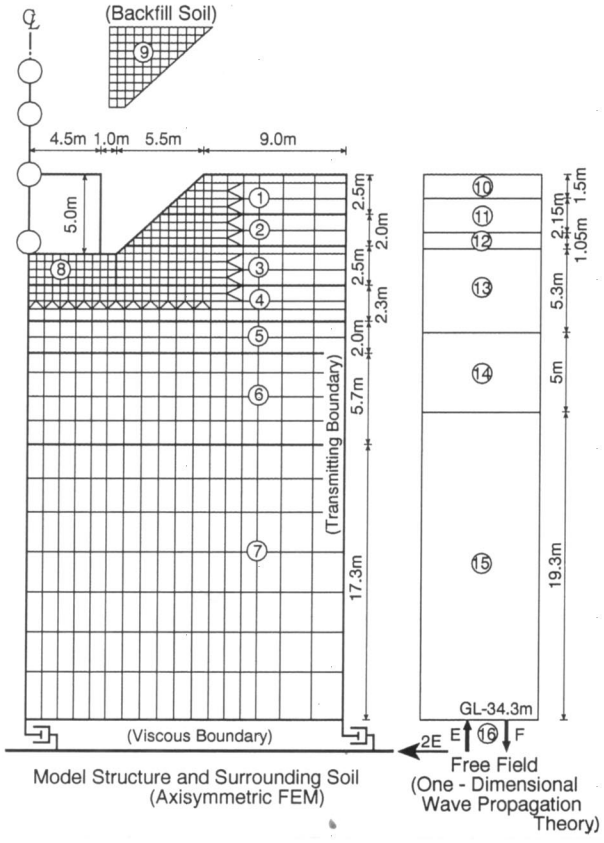

Fig.2. Analysis model

Table 1. Soil constants for analysis

(a) Surrounding soil					(b) Free field			
No.	ρ (t/m³)	V_S (m/sec.)	ν	h (%)	No.	ρ (t/m³)	V_S (m/sec.)	h (%)
①	1.5	140	0.39	5	⑩	1.7	100	5
②	1.7	270	0.29	5	⑪	1.7	220	5
③	1.7	340	0.34	5	⑫	1.8	270	5
④	1.7	400(450)	0.12	3	⑬	1.9	340	5
⑤	1.7	400(450)	0.46(0.41)	3	⑭	1.9	520	5
⑥	1.9	1330	0.11	3	⑮	1.9	1250	5
⑦	2.1	1600	0.35	3	⑯	2.1	1600	3
⑧	1.7	230(270)	0.12	5				
⑨	1.7-1.8	110-150	0.30	2-4				

ρ : Mass density; V_S : Shear wave velocity; ν : Poisson's ratio; h : Damping factor
(The values in parentheses show the values for Model B)

FORCED VIBRATION TEST RESULTS

Table 2 shows the resonance frequency, peak amplitude, damping factor and displacement ratios to the top horizontal displacement at resonance frequency for RF excitation. It is confirmed that the resonance frequency and damping increase, and peak amplitude decreases due to the embedment effect. The sway ratio in the displacement at RF for RF excitation is not sensitive to the embedment effect, but the rocking ratio decreases and the elastic deformation ratio of the structure increases with embedment.

The relation between the shearing force and moment at the foundation bottom and the corresponding displacement during the forced vibration test is expressed in the following formula :

$$\begin{Bmatrix} Q \\ M \end{Bmatrix} = \begin{Bmatrix} K_H u_0 \\ K_R \theta_0 \end{Bmatrix} = \begin{bmatrix} K_{HH} & K_{HR} \\ K_{RH} & K_{RR} \end{bmatrix} \begin{Bmatrix} u_0 \\ \theta_0 \end{Bmatrix} \quad (1)$$

where Q, M: shearing force and moment; u_0, θ_0: horizontal and rotational displacement; K_H, K_R: combined horizontal and rotational impedance functions at foundation bottom; K_{HH}, K_{RR}, $K_{HR} = K_{RH}$: dynamic impedance functions. The combined impedance functions (K_H, K_R) were calculated directly using the test results. The dynamic impedance functions (K_{HH}, K_{RR}, $K_{HR} = K_{RH}$) were then derived from the data (K_H, K_R, u_0 and θ_0) for RF and 1F excitations using the method of least squares (Ohtsuka et al., 1992).

Fig.3 shows the comparison of the dynamic soil impedance functions for both models. In the analysis, the basement without the superstructure was modeled as being massless and rigid. The embedment effect is to increase the real and imaginary parts with embedment and to complicate the dynamic characteristics because of the influence of the backfill soil and the surrounding soil. The analytical results show good agreement with the test results.

Fig.4 compares the horizontal displacement resonance curves at the RF and 1F of both models for the RF excitation. Two peaks in the test results for Model A are considered to be caused by the orthogonal vibration (with respect to the direction of forced vibration) due to inhomogeneity of the soil underneath the foundation bottom. The peak amplitude decreases and the resonance frequency increases due to the embedment effect. The analytical results correspond to the test results of the resonance curves as a whole, except the resonance peaks of Model A.

EARTHQUAKE OBSERVATION RESULTS

Four earthquake records were used. Table 3 shows the outline of these earthquakes, and Fig.5 shows their epicenters in relation to the observation site. Their maximum accelerations on the surface of the free field, except that of EQ4, were almost the same.

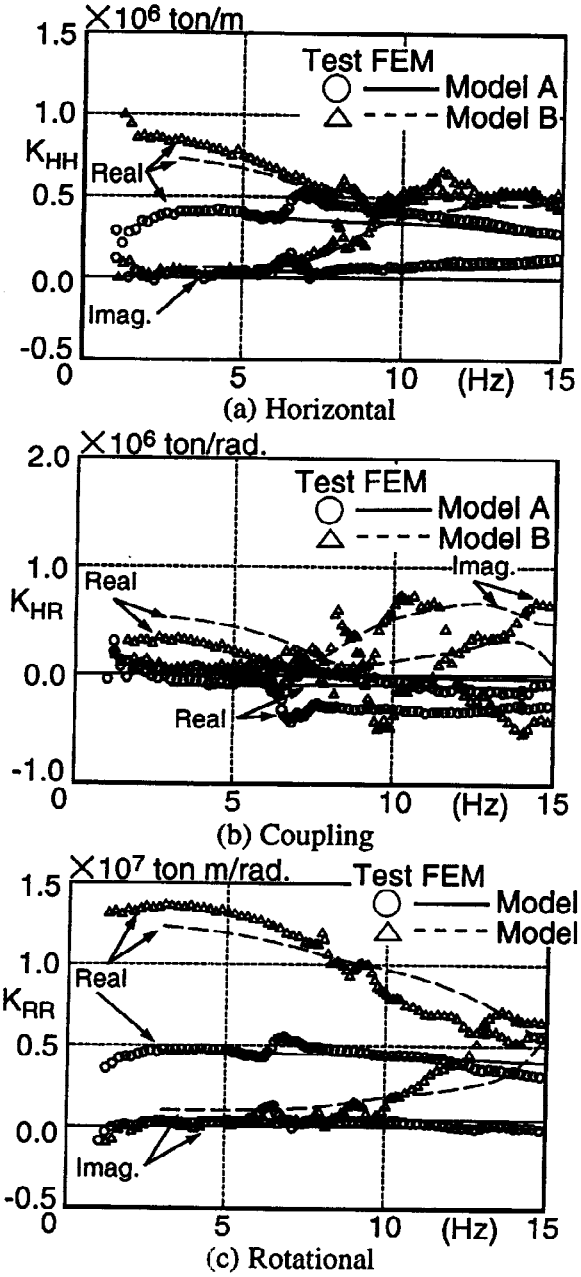

Fig.3. Comparison of dynamic soil impedance functions

Table 2. Test results for RF excitation

		Model A	Model B
Resonance frequency (Hz)		6.3	9.2
Peak amplitude on RF (μm/ton)		190	49
Damping factor on RF (%)		9.4	13.5
Displacement ratios (%)	Sway	14	14
	Rocking	77	72
	Deformation of structure	9	14

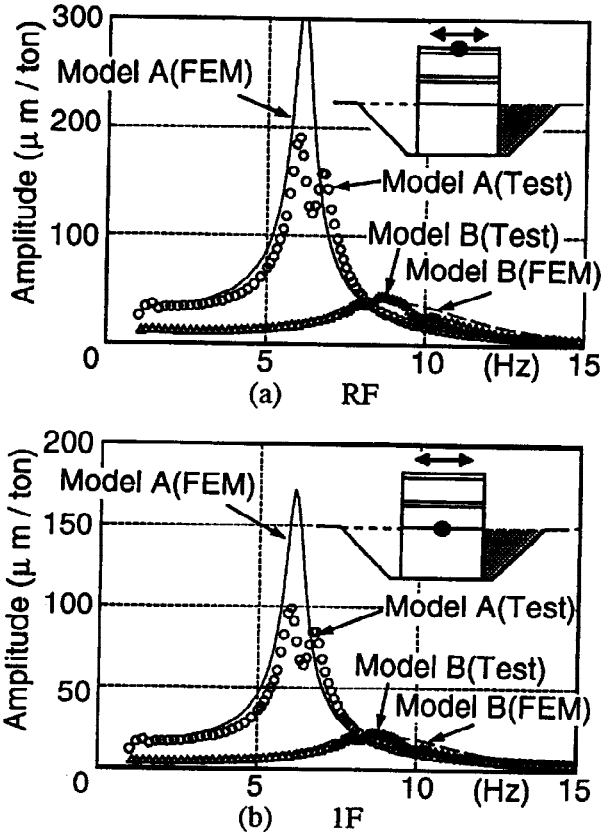

Fig.4. Comparison of horizontal displacement resonance curves for RF excitation

Table 3. Outline of observed Earthquakes

EQ No.	Date	M	D (km)	X (km)	Δ (km)	Amax (Gal)
1	Nov. 2, 1989	7.1	0	206	206	26.2
2	Nov. 2, 1990	5.7	76	102	69	24.5
3	Mar. 5, 1991	4.0	37	46	28	15.8
4	Jul. 12, 1992	6.5	90	105	54	60.4

M : Magnitude; D : Depth; X : Hypocentral distance;
Δ : Epicentral distance; Amax : Maximum horizontal (NS) acceleration on surface of free field

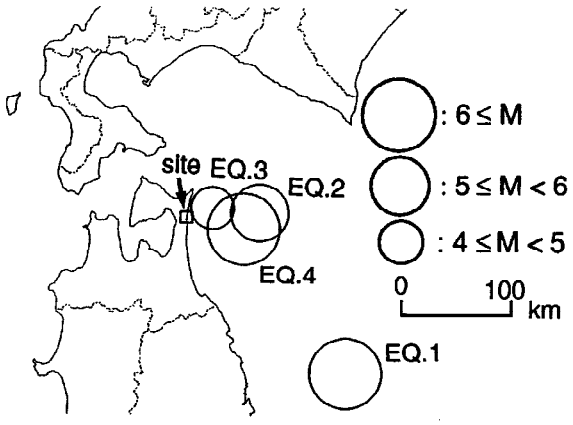

Fig.5. Epicenters of earthquakes and site location

Fig.6 compares the Fourier spectra of horizontal accelerations on the top of the two models. It is clarified that the spectrum amplitude decreases and the predominant frequency increases due to the embedment effect. Furthermore, these differences do not depend on the characteristics of earthquake records. It appears that two peaks in the horizontal resonance curve of Model A are also recognized in the Fourier spectrum of accelerations for Model A, while differences are shown between the resonance frequency in Fig.4 and the predominant frequency in Fig.6. The horizontal and rotational foundation input motions were calculated using the dynamic impedance functions obtained from the forced vibration test results and earthquake records of the structures for Models A and B, and substituting those into the following equation.

$$\begin{Bmatrix} u^* \\ \theta^* \end{Bmatrix} = \begin{Bmatrix} u_0 \\ \theta_0 \end{Bmatrix} + \begin{bmatrix} K_{HH} & K_{HR} \\ K_{RH} & K_{RR} \end{bmatrix}^{-1} \begin{Bmatrix} Q \\ M \end{Bmatrix} \tag{2}$$

where u^*, θ^* are the horizontal and rotational components of foundation input motion (Fukuoka et al., 1995).

Fig.7 shows the foundation input motions normalized by the response on the surface of the free field. This figure also compares the analytical results and the observed results. In the analysis, the basement without the superstructure was modeled as being massless and rigid, and the incident seismic wave was assumed to be a vertically propagating plane SH wave. The foundation input motions for those earthquakes indicate a similar frequency characteristic. The horizontal components decrease with increasing frequency, but increase in the high frequency range. The rotational ones are small in the low frequency range and increase in the high frequency range. The fluctuation in the foundation input motions for the embedment depends on frequency. In the vicinity of the natural frequency of the subsurface soil, the foundation input motions for embedded structures are greater than for non-embedded structures. It seems that the foundation input motions for the embedded structure are influenced by amplification of earthquake motion in the subsurface soil. The analytical results show generally good agreement with the observed ones, although differences are recognized in the higher frequency range.

Fig.8 compares the transfer functions of analytical accelerations for Models A and B (both basements without the superstructures were modeled as being massless and rigid) and the free field. Both transfer functions are defined by the amplifications at the center of the basement due to incident plane SH waves. For the free field, the transfer function is defined by the inverse of amplification on the surface of the free field due to incident plane SH waves. It is confirmed that the discrepancies of the foundation input motions, in the vicinity of the natural frequency of the subsurface soil, between the embedment model and the non-embedment model are due to the amplification of earthquake motion in the subsurface soil.

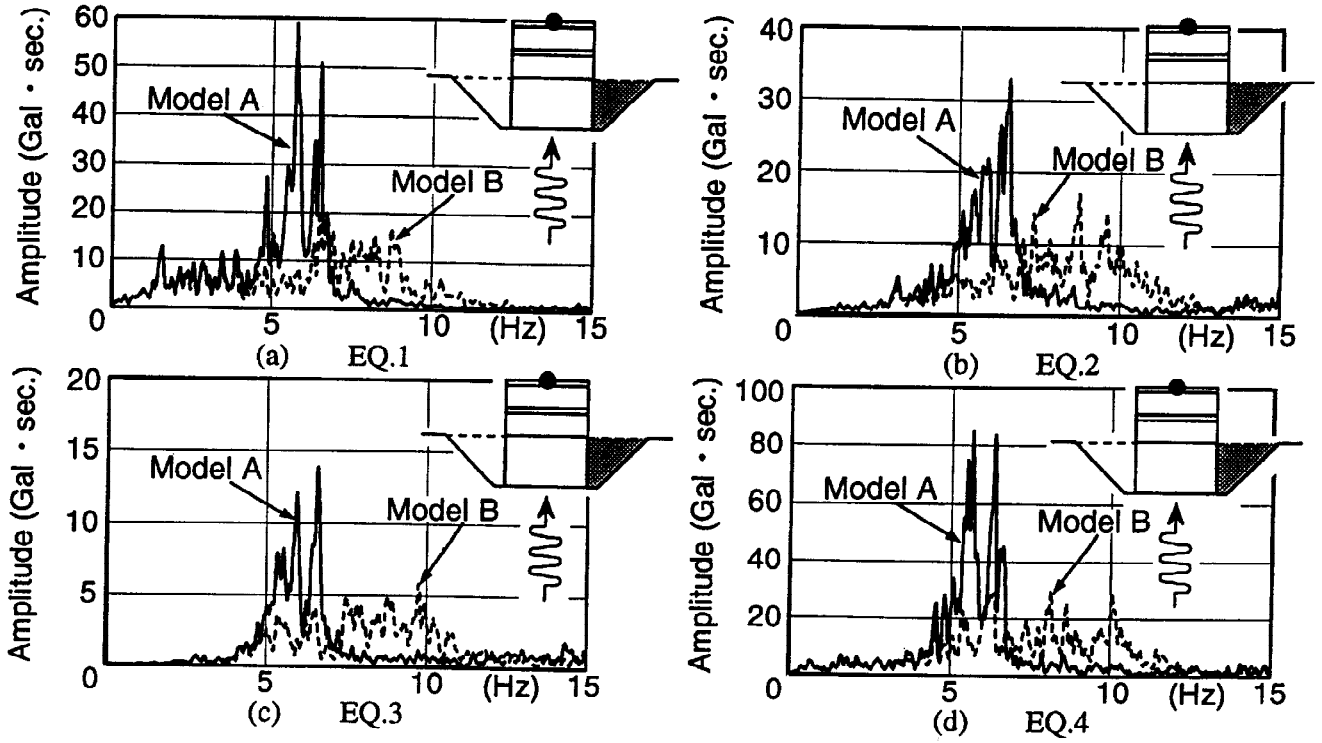

Fig.6. Comparison of Fourier spectra of horizontal accelerations on RF

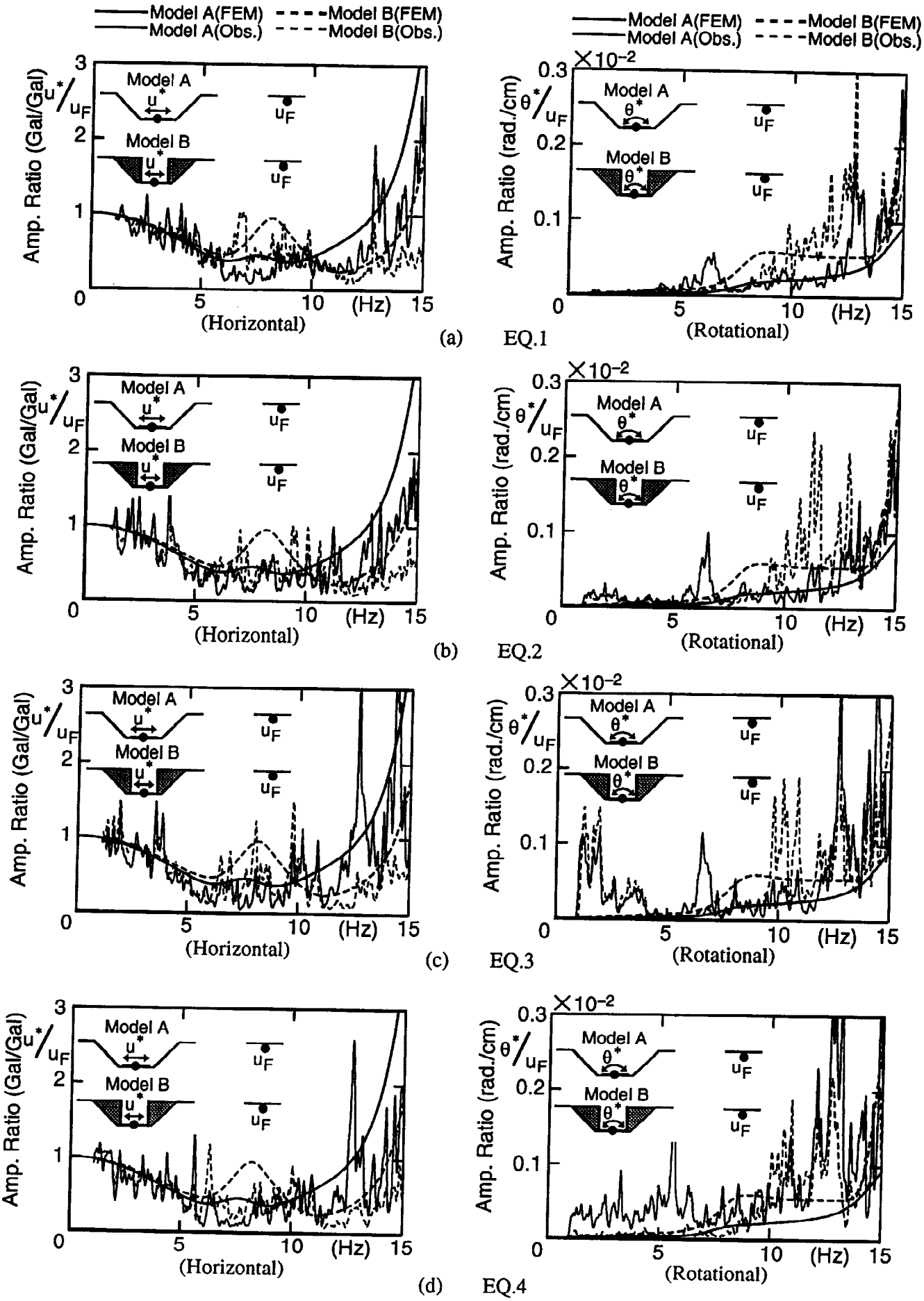

Fig.7. Comparison of foundation input motions

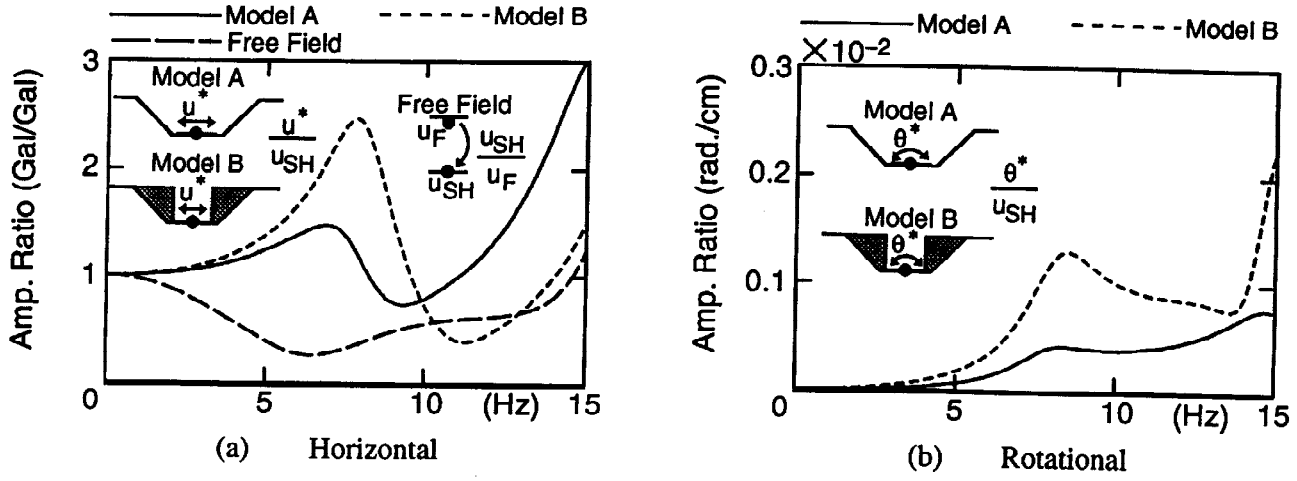

Fig.8. Comparison of transfer functions

Fig.9 compares the absolute-displacement mode due to the incident plane SH wave normalized by the amplitude of the incident wave. Each frequency is the predominant frequency of the horizontal input motion (Fig.7). It is clarified that the absolute displacements at the center of the basement and the surface of the surrounding soil for the embedded model are greater than those of the non-embedded model. It seems that the amplification of earthquake motion in the backfill soil increases the foundation input motion for the embedded model.

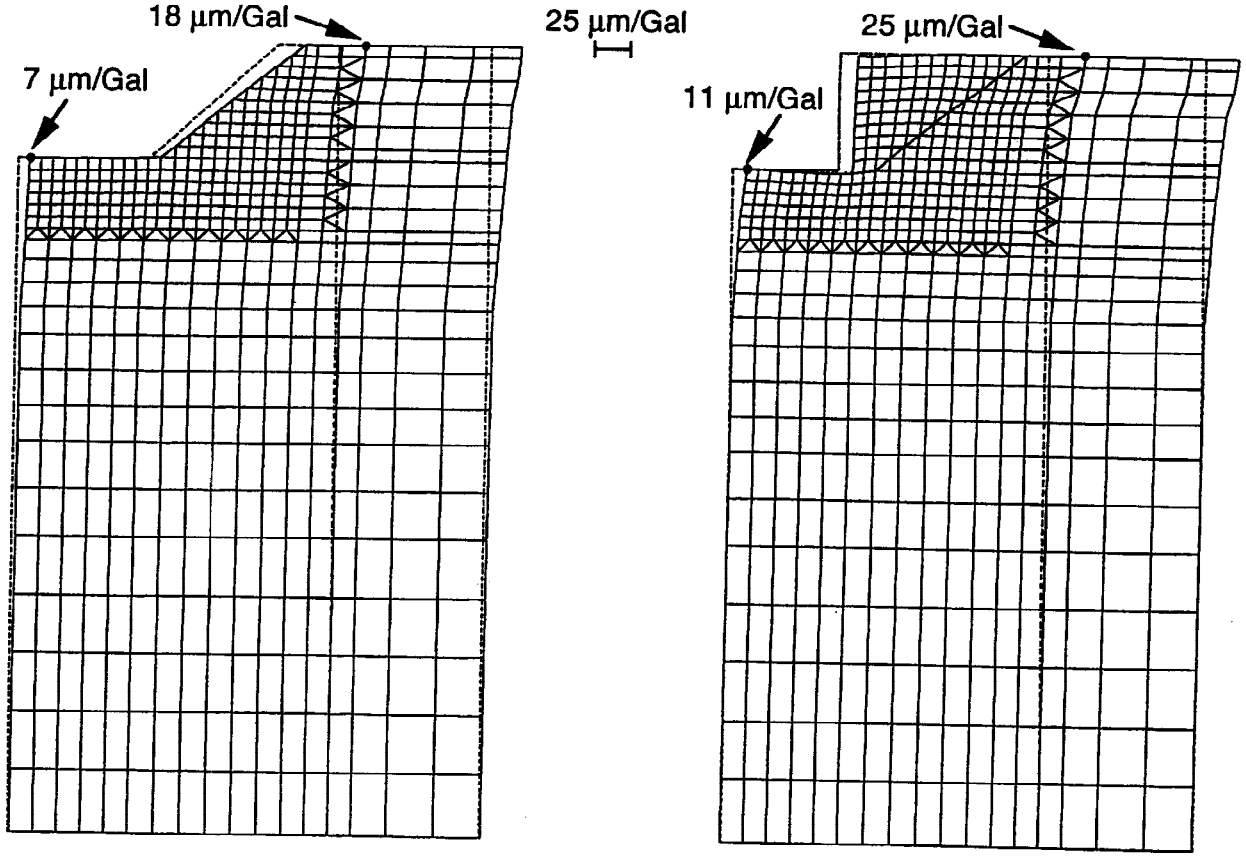

(a) Non-embedded model (6.8 Hz) (b) Embedded model (7.8 Hz)

Fig.9. Comparison of absolute-displacement mode due to incident plane SH waves

CONCLUSIONS

Forced vibration tests and earthquake observations were carried out on large-scale models constructed on ground to investigate the inertial and kinematic interactions of embedded structures. For the forced vibration tests, the structure responses were measured and dynamic soil impedances were evaluated. Using the dynamic soil impedances and earthquake observation records for the structures, the foundation input motions were also calculated. For the dynamic soil impedances and the foundation input motions, correlation analyses were worked out using Axisymmetric FEM. Concluding remarks of this study are as follows:

1. The real and imaginary parts of the dynamic soil impedance increase due to the embedment and its dynamic characteristics become more complicated.
2. The resonance frequency of soil-structure systems increases due to the embedment, and the resonance amplitude decreases.
3. The rocking component ratio decreases and the ratio of elastic deformation increases with the embedment, but the sway component ratio is not sensitive to the embedment.
4. The Fourier spectra of horizontal accelerations of the test models show that the amplitude decreases and the predominant frequency becomes higher with the embedment.
5. In the vicinity of the natural frequency of the subsurface soil, the foundation input motions for the embedded structures are greater than those for non-embedded structures.
6. Axisymmetric FEM models are useful for investigating the inertial and kinematic interaction of the embedded structures.

ACKNOWLEDGMENTS

This work was carried out by the Nuclear Power Engineering Corporation (NUPEC) as an entrusted project sponsored by the Ministry of International Trade and Industry in Japan. This work was supported by "Committee of Model Tests of Embedment Effect on Reactor Buildings" of NUPEC. The authors wish to express their gratitude for the cooperation and valuable suggestions given by the members of the Committee.

REFERENCES

Fukuoka, A., et al. (1995). Dynamic soil-structure interaction of embedded structure. *Proc. 13th SMiRT*, III, 85-90.

Miyamoto, Y., et al. (1991). Experimental studies on an embedded structure-soil interaction. *Proc. Second International Conference on Recent Advances in Geotechnical Earthquake Engineering and Soil Dynamics*, 1, 845-852.

Ohtsuka, Y., et al. (1992). Embedment effects on dynamic soil-structure interaction. *Proc. 10th WCEE*, 3, 1707-1712.